JOURNAL OF COMPUTATIONAL PHYSICS 30, 407–427 (1979)

Computer Model for Bounded Plasma

VIKTOR K. DECYK AND JOHN M. DAWSON

Department of Physics, University of California, Los Angeles, California 90024

Received December 19, 1977; revised April 4, 1978

A computer model is developed for simulating a bounded plasma slab. The two dimensional electrostatic model is periodic in one dimension and bounded in the other. In the non-periodic dimension, one can specify values of the potential or the normal electric field on both boundaries, or one can specify that a vacuum exists outside the plasma or any combination of these on each boundary. The plasma model can be non-neutral. Because the final solution has a particularly simple form, it can be obtained with only one Fast Fourier Transform, and therefore this model is only slightly slower than conventional doubly periodic models. External electrostatic sources, either on the boundaries or in the plasma interior, can be added in a natural way. The computer model is tested by examining the propagation of linear waves in a plasma slab bounded by vacuum. The predictions of a dispersion relation based on a warm fluid model are compared with the results obtained from the computer model, with very good agreement for the real parts of the frequencies.

I. INTRODUCTION

Until recently most electrostatic plasma simulation models with more than one spatial dimension have been doubly periodic. There are a number of reasons for this. From the point of view of investigating plasma theory, one is often interested in basic plasma phenomena without the additional difficulty of having boundary effects to consider. Periodic models satisfy this need because linear dispersion for such a model differs from that of an infinite plasma only by the discrete set of wavenumbers allowed in the former. Further, many nonlinear phenomena are not affected by periodicity. Finally, there exist efficient algorithms for solving Poisson's equation [1, 2] which make use of the Fast Fourier Transform (FFT) [3], and these are naturally suited for periodic systems.

There are many problems in plasma physics, however, where boundary conditions are important. There are problems in plasma sheaths, plasma confinement, penetration of electric fields, and heating of plasmas by external sources to name just a few. Further, plasma simulation is most valuable when it can model real experiments, where boundary conditions are usually unavoidable. Finally, the ability to more accurately simulate fusion devices will eventually be a necessity.

Although solutions to Poisson's equation are known analytically for a variety of boundary value problems, these are not useful computationally in a major plasma simulation because a great deal of computing would be required at each time step.

0021-9991/79/030407-21$02.00/0

There exists as yet no Fast Bessel Transform, for example, which is equivalent in speed to the FFT. The usual approach in such problems has been to solve a finite-difference form of Poisson's equation at a fixed number of field points, such as the five-point difference equation in two dimensions,

$$\frac{\Phi(x+\delta, y) - 2\Phi(x, y) + \Phi(x-\delta, y)}{\delta^2} + \frac{\Phi(x, y+\delta) - 2\Phi(x, y) + \Phi(x, y-\delta)}{\delta^2}$$

$$= -4\pi\rho(x, y). \tag{1}$$

This approximate equation can be solved exactly. Efficient algorithms exist [4] which solve Poisson's equation in two dimensions when either the potential is specified or the normal derivative vanishes on the boundaries. With more complicated boundary conditions, solutions are more difficult to obtain because the resulting system of equations is in quindiagonal form [5], although clever algorithms have been devised for some cases [4, 6]. A special case of interest in plasma simulation models occurs when the system is periodic in one direction. By performing a discrete Fourier analysis on the two-dimensional five-point difference equation, one obtains a three-point difference equation in one dimension for each Fourier mode [7]. Efficient algorithms for solving the resulting set of tridiagonal matrices for generalized boundary conditions exist [5] and for special cases the algorithms have been optimized [7, 8].

We present here an alternative yet systematic approach to electrostatic boundary value problems which involves the use of Fourier series. The philosophy behind this approach is that we look for an approximate solution to a differential equation rather than an exact solution of a finite-difference equation. In this method, the contribution to the potential Φ from the charges is first found for a doubly periodic system. This is the most timeconsuming part of the calculation and there already exist efficient algorithms for performing it [9]. One then adds appropriate solutions of Laplace's equation, which can be found analytically, such that the sum of the two solutions satisfies the given boundary conditions. This approach can be applied to various geometries, but the case of a slab which is periodic in one dimension is particularly simple. In that case, one can obtain an exact solution in terms of an infinite Fourier series. The approximation consists of truncating the infinite sum and only approximating the Fourier coefficients of the charge density. If Φ is evaluated only at fixed field points and interpolated in an appropriate fashion between them, one can use the FFT to perform the calculation. The result is that only a slight increase in computing time is necessary to simulate a bounded system compared to a doubly periodic system. Because the solutions are found in k space, many of the techniques which have been developed over the years for periodic systems can still be applied in this model. Finite-size particles are treated very simply by a convolution theorem. Additional smoothing, if desired, can be done in k space. Electrostatic antennas, or capacitor plates, can be added to the model in a natural way. Finally, existing doubly periodic codes which use Fourier series can be modified without major changes to include the effects of boundaries.

II. Solution to Poisson's Equation for Doubly Periodic Systems

Poisson's equation in two dimensional rectangular co-ordinates has the form:

$$\frac{\partial^2 \Phi}{\partial x^2} + \frac{\partial^2 \Phi}{\partial y^2} = -4\pi\rho \tag{2}$$

Taking the Fourier integral and integrating by parts gives:

$$\begin{aligned}
&\frac{1}{L_x L_y}\int_0^{L_x}\int_0^{L_y} \nabla^2\Phi e^{-ik_n x} e^{-ik_m y}\, dx\, dy \\
&\quad = \frac{1}{L_x L_y}\int_0^{L_y} \left\{\frac{\partial \Phi}{\partial x} + ik_n \Phi\right\}\Big|_{x=0}^{x=L_x} e^{-ik_m y}\, dy \\
&\qquad + \frac{1}{L_x L_y}\int_0^{L_x} \left\{\frac{\partial \Phi}{\partial y} + ik_m \Phi\right\}\Big|_{y=0}^{y=L_y} e^{-ik_n x}\, dx - (k_n{}^2 + k_m{}^2)\, \Phi_{nm} \\
&\quad = -4\pi\rho_{nm}\,,
\end{aligned} \tag{3}$$

where the Fourier coefficient in two dimensions is defined by

$$f_{nm} \equiv \frac{1}{L_x L_y}\int_0^{L_x}\int_0^{L_y} f(x, y)\, e^{-ik_n x} e^{-ik_m y}\, dx\, dy, \tag{4}$$

and $k_n = 2n\pi/L_x$, $k_m = 2m\pi/L_y$. One can see that if Φ and its normal derivative are periodic at the boundaries, then Poisson's equation in Fourier space is:

$$(k_n{}^2 + k_m{}^2)\, \Phi_{nm} = 4\pi\rho_{nm}\,. \tag{5}$$

From (5) it follows that one must have $\rho_{00} = 0$ for a periodic system. That is, the overall system must be electrically neutral. The solution can be inverted immediately:

$$\Phi(x, y) = \sum_{n,m=-\infty}^{\infty}{}' \frac{4\pi\rho_{nm}}{k_n{}^2 + k_m{}^2}\, e^{ik_n x} e^{ik_m y}, \tag{6}$$

where the prime indicates that $m = n = 0$ is omitted from the sum. The arbitrary constant Φ_{00} has been set equal to zero.

III. Solution to Poisson's Equation for *SLAB* Geometry

If Φ is not periodic, then (3) is an integro-differential equation for Φ with unknown solution. There is a special case, however, that can be treated simply. If Φ and its normal derivative are periodic in one direction, let us call that the y direction, then

the Fourier integral of Poisson's equation in the y direction gives the following differential equation:

$$\frac{d^2\Phi_n(x)}{dx^2} - k_m{}^2\Phi_m(x) = -4\pi\rho_m(x). \tag{7}$$

The solution of this equation can be constructed from any particular solution plus the solution of the homogeneous equation which is chosen to satisfy the appropriate boundary conditions. For $m \neq 0$, a particular solution has already been found, namely the periodic solution, and the solution to the homogeneous equation is a combination of positive and negative exponentials. Thus we have for $m \neq 0$,

$$\Phi_m(x) = \psi_m(x) + A_m e^{k_m x} + B_m e^{-k_m x}, \tag{8}$$

where

$$\psi_m(x) = \sum_{n=-m}^{\infty} \frac{4\pi\rho_{nm}}{k_n{}^2 + k_m{}^2} e^{ik_n x} \tag{9}$$

is the periodic solution and A_m, B_m are constants chosen to satisfy the boundary conditions. For the case $m = 0$, we want to include the possibility that the system is not electrically neutral. In that case an appropriate solution is:

$$\Phi_0(x) = \psi_0(x) + 2\pi\rho_{00}x(L_x - x) + A_0 x + B_0, \tag{10}$$

where

$$\psi_0(x) = \sum_{n=-\infty}^{\infty}{}' \frac{4\pi\rho_{n0}}{k_n{}^2} e^{ik_n x}, \tag{11}$$

and the prime indicates that $n = 0$ is omitted from the sum. The general solution is then found by forming the Fourier series in the y direction:

$$\Phi(x, y) = \sum_{m=-\infty}^{\infty} \Phi_m(x) e^{ik_m y}. \tag{12}$$

The electric field in the x and y directions is found by straightforward differentiation:

$$E_m{}^x(x) = -\frac{d\Phi_m(x)}{dx} \quad \text{and} \quad E_m{}^y(x) = -ik_m\Phi_m(x). \tag{13}$$

Boundary conditions can be expressed in the following generalized form:

$$\alpha_m(0)\,\Phi_m(0) + \beta_m(0)\frac{d\Phi_m(0)}{dx} = \gamma_m(0) \tag{14}$$

$$\alpha_m(L_x)\,\Phi_m(L_x) + \beta_m(L_x)\frac{d\Phi_m(L_x)}{dx} = \gamma_m(L_x), \tag{15}$$

where α_m, β_m, and γ_m are constants appropriate to the boundary conditions at $x = 0$, and $x = L_x$. Substituting equation (8) into (14) and (15) yields the equations which determine the constants A_m, B_m:

$$\alpha_m(0)\{\psi_m(0) + A_m + B_m\} + \beta_m(0)\left\{\frac{d\psi_m(0)}{dx} + k_m A_m - k_m B_m\right\} = \gamma_m(0), \tag{16}$$

$$\alpha_m(L_x)\{\psi_m(L_x) + A_m e^{k_m L_x} + B_m e^{-k_m L_x}\} + \beta_m(L_x)\left\{\frac{d\psi_m(L_x)}{dx} + k_m A_m e^{k_m L_x} - k_m B_m e^{-k_m L_x}\right\} = \gamma_m(L_x). \tag{17}$$

After solving for A_m, B_m one can express the solution (8) in the following form:

$$\Phi_m(x) = \psi_m(x) + G_m(0)\,\chi_m{}^L(x) + G_m(L_x)\,\chi_m{}^R(x), \tag{18}$$

where we define the following constants:

$$G_m(0) = \gamma_m(0) - \alpha_m(0)\,P_m + \beta_m(0)\,\Pi_m \tag{19}$$

$$G_m(L_x) = \gamma_m(L_x) - \alpha_m(L_x)\,P_m + \beta_m(L_x)\,\Pi_m \tag{20}$$

$$P_m = \psi_m(0) = \psi_m(L_x) = \sum_{n=-\infty}^{\infty} \frac{4\pi\rho_{nm}}{k_n{}^2 + k_m{}^2} \tag{21}$$

$$\Pi_m = -\frac{d\psi_m(0)}{dx} = -\frac{d\psi_m(L_x)}{dx} = \sum_{n=-\infty}^{\infty} -\frac{ik_n}{k_n{}^2 + k_m{}^2}\,4\pi\rho_{nm} \tag{22}$$

$$\chi_m{}^L(x) = \{\alpha_m(L_x)\sinh[k_m(L_x - x)] + k_m\beta_m(L_x)\cosh[k_m(L_x - x)]\}/N_m \tag{23}$$

$$\chi_m{}^R(x) = \{\alpha_m(0)\sinh(k_m x) - k_m\beta_m(0)\cosh(k_m x)\}/N_m \tag{24}$$

$$N_m = [\alpha_m(0)\,\alpha_m(L_x) - k_m{}^2\beta_m(0)\,\beta_m(L_x)]\sinh(k_m L_x) + k_m[\alpha_m(0)\,\beta_m(L_x) - \alpha_m(L_x)\,\beta_m(0)]\cosh(k_m L_x). \tag{25}$$

The quantitites $\chi_m{}^L(x)$ and $\chi_m{}^R(x)$ depend only on the type of boundary conditions, and therefore can be calculated once at the beginning of the simulation and stored. The quantities $G_m(0)$ and $G_m(L_x)$ must be updated each time, but their calculation involves only simple sums and products.

For the case $m = 0$, we shall still express the boundary conditions in the form of equations (14) and (15). However, all the constants cannot be arbitrarily specified because Gauss' Law must be satisfied in two dimensions,

$$4\pi \int_A \rho\, dA = -\oint_C \frac{\partial\Phi}{\partial n}\, dl. \tag{26}$$

When the system is periodic in the y direction, this condition can be expressed:

$$4\pi\rho_{00}L_xL_y = -\int_0^{L_y}\left\{\sum_{m=-\infty}^{\infty}\frac{d\Phi_m(x)}{dx}\right\}\Bigg|_{x=0}^{x=L_x} e^{ik_m y}\,dy = -\frac{d\Phi_0(x)}{dx}\Bigg|_{x=0}^{x=L_x}\cdot L_y \quad (27)$$

Thus the constants α_0, β_0, and γ_0 in (14) and (15) must be chosen to be consistent with the requirement:

$$\frac{d\Phi_0(L_x)}{dx} - \frac{d\Phi_0(0)}{dx} + 4\pi\rho_{00}L_x = 0 \quad (28)$$

Substituting equation (10) into (14) and (15) yields the equations which determine the constants A_0, B_0:

$$\alpha_0(0)\{\psi_0(0) + B_0\} + \beta_0(0)\left\{\frac{d\psi_0(0)}{dx} + 2\pi\rho_{00}L_x + A_0\right\} = \gamma_0(0), \quad (29)$$

$$\alpha_0(L_x)\{\psi_0(L_x) + A_0L_x + B_0\} + \beta_0(L_x)\left\{\frac{d\psi_0(L_x)}{dx} - 2\pi\rho_{00}L_x + A_0\right\} = \gamma_0(L_x). \quad (30)$$

After solving for A_0, B_0, equation (10) can be written in the form:

$$\Phi_0(x) = \psi_0(x) + 2\pi\rho_{00}x(L_x - x) + G_0(0)\,\chi_0{}^L(x) + G_0(L_x)\,\chi_0{}^R(x) - P_0, \quad (31)$$

where we define the following constants:

$$G_0(0) = \gamma_0(0) + \beta_0(0)[\Pi_0 - 2\pi\rho_{00}L_x] \quad (32)$$

$$G_0(L_x) = \gamma_0(L_x) + \beta_0(L_x)[\Pi_0 + 2\pi\rho_{00}L_x] \quad (33)$$

$$P_0 = \sum_{n=-\infty}^{\infty}{}' \frac{4\pi\rho_{n0}}{k_n{}^2} \quad (34)$$

$$\Pi_0 = \sum_{n=-\infty}^{\infty}{}' -\frac{i}{k_n}4\pi\rho_{n0} \quad (35)$$

$$\chi_0{}^L(x) = [\alpha_0(L_x)(L_x - x) + \beta_0(L_x)]/N_0 \quad (36)$$

$$\chi_0{}^R(x) = [\alpha_0(0)\,x - \beta_0(0)]/N_0 \quad (37)$$

$$N_0 = \alpha_0(0)\,\beta_0(L_x) - \alpha_0(L_x)\,\beta_0(0) + \alpha_0(0)\,\alpha_0(L_x)\,L_x\,. \quad (38)$$

If programming simplicity is more important than computational efficiency, these equations can be programmed as they stand. In the following subsections we examine some special cases, deriving the appropriate constants to properly formulate the boundary conditions and expressing the simplified form of the solution which may allow some optimization in storage and calculation.

1. *Potential specified at* $x = 0, L_x$.

This case is straightforward, with $\alpha_m(0) = \alpha_m(L_x) = 1$, $\beta_m(0) = \beta_m(L_x) = 0$, and where we define:

$$\gamma_m(0) = \phi_m(0) = \frac{1}{L_y}\int_0^{L_y} \Phi(0, y)\, e^{-ik_m y}\, dy, \tag{39}$$

$$\gamma_m(L_x) = \phi_m(L_x) = \frac{1}{L_y}\int_0^{L_y} \Phi(L_x, y)\, e^{-ik_m y}\, dy. \tag{40}$$

The functions $\chi_m(x)$ have the simplifying feature that $\chi_m{}^R(L_x - x) = \chi_m{}^L(x)$. The solutions can be written in the form:

$$\Phi_m(x) = \psi_m(x) + \{[\phi_m(L_x) - P_m] \sinh(k_m x) + [\phi_m(0) - P_m] \sinh[k_m(L_x - x)]\}/\sinh(k_m L_x) \tag{41}$$

$$\Phi_0(x) = \psi_0(x) + 2\pi\rho_{00}x(L_x - x) + [\phi_0(L_x) - P_0]\left(\frac{x}{L_x}\right) + [\phi_0(0) - P_0]\left(1 - \frac{x}{L_x}\right). \tag{42}$$

These solutions can be used to model the particularly interesting case of a plasma bounded by conducting walls by setting $\Phi = 0$ at the boundaries. With conducting walls one could also expand the potential directly in terms of the eigenmodes $\sin(n\pi x/L_x)$. However, the expansion in terms of eigenmodes requires twice as many modes and therefore more calculation to achieve the same resolution as the method presented here. With the present method, the case when the plasma has driven antennas on the boundaries can also be modeled by specifying the potentials on the boundaries as functions of time.

2. *Normal electric field specified at* $x = 0, L_x$.

In this case we have for $m \neq 0$, $\alpha_m(0) = \alpha_m(L_x) = 0$, $\beta_m(0) = \beta_m(L_x) = -1$, and we define:

$$\gamma_m(0) = \epsilon_m(0) = -\frac{1}{L_y}\int_0^{L_y} \frac{\partial\Phi(0, y)}{\partial x}\, e^{-ik_m y}\, dy, \tag{43}$$

$$\gamma_m(L_x) = \epsilon_m(L_x) = -\frac{1}{L_y}\int_0^{L_y} \frac{\partial\Phi(L_x, y)}{\partial x}\, e^{-ik_m y}\, dy. \tag{44}$$

The functions $\chi_m(x)$ have the property that $\chi_m{}^R(L_x - x) = -\chi_m{}^L(x)$, and the solution can be written in the form:

$$\Phi_m(x) = \psi_m(x) - \{[\epsilon_m(L_x) - \Pi_m] \cosh(k_m x) - [\epsilon_m(0) - \Pi_m] \cosh[k_m(L_x - x)]\}/k_m \sinh(k_m L_x). \tag{45}$$

For the case $m = 0$, boundary constants which are consistent with the restriction of Gauss' Law are: $\alpha_0(0) = 1$, $\alpha_0(L_x) = 0$, $\beta_0(0) = \beta_0(L_x) = -1$, and:

$$\gamma_0(0) = \epsilon_0(L_x) - 4\pi\rho_{00}L_x + \Phi_0(0) \tag{46}$$

$$\gamma_0(L_x) = \epsilon_0(L_x) \tag{47}$$

The solution is then determined to within the constant $\Phi_0(0)$:

$$\Phi_0(x) = \psi_0(x) + 2\pi\rho_{00}x(L_x - x) - [\epsilon_0(L_x) - \Pi_0 - 2\pi\rho_{00}L_x]x + \Phi_0(0) - P_0 . \tag{48}$$

Since Gauss' Law determines $\epsilon_0(0)$ once $\epsilon_0(L_x)$ is specified, $\epsilon_0(0)$ does not enter in (48).

3. *Potential specified at $x = 0$, normal electric field at $x = L_x$.*

For this case one has $\alpha_m(0) = 1$, $\alpha_m(L_x) = \beta_m(0) = 0$, $\beta_m(L_x) = -1$, and $\gamma_m(0) = \phi_m(0)$, $\gamma_m(L_x) = \epsilon_m(L_x)$, and the solution can be written in the form:

$$\Phi_m(x) = \psi_m(x) - \{[\epsilon_m(L_x) - \Pi_m] \sinh(k_m x) - [k_m\phi_m(0) - k_m P_m] \cosh[k_m(L_x - x)]\}/k_m \cosh(k_m L_x). \tag{49}$$

For $m = 0$, one obtains equation (48).

4. *Vacuum specified at $x = 0$, L_x.*

A situation of particular interest is an isolated plasma with vacuum on the outside. We thus consider here the problem of an isolated slab, which is periodic in the y direction, with no charge extending outside the interior region $0 \leqslant x \leqslant L_x$. The solution in the interior region is still given by (8) and (10). In the exterior regions, the appropriate differential equation is:

$$\frac{d^2\Phi_m{}^v(x)}{dx^2} - k_m{}^2\Phi_m{}^v(x) = 0. \tag{50}$$

The vacuum solutions must not grow exponentially away from the boundaries so that the appropriate solutions are:

$$\Phi_m{}^v(x) = \Phi_m(0)\, e^{|k_m|x} \qquad x \leqslant 0, \tag{51}$$

$$\Phi_m{}^v(x) = \Phi_m(L_x)\, e^{|k_m|(L_x - x)} \qquad x \geqslant L_x . \tag{52}$$

where we have already required that Φ_m be continuous across the boundary. From Gauss' Law one can show that the jump in the normal component of the electric

field is given by any external surface charge density on the boundary, $\Delta E_n = 4\pi\sigma_{\text{ext}}$. If one defines

$$\sigma_m(0) = \frac{1}{L_y}\int_0^{L_y} \sigma_{\text{ext}}(0, y)\, e^{-ik_m y}\, dy, \tag{53}$$

$$\sigma_m(L_x) = \frac{1}{L_y}\int_0^{L_y} \sigma_{\text{ext}}(L_x, y)\, e^{-ik_m y}\, dy. \tag{54}$$

then one can show that the appropriate boundary conditions are:

$$-\frac{d\Phi_m(0)}{dx} + |k_m|\,\Phi_m(0) = 4\pi\sigma_m(0), \tag{55}$$

$$\frac{d\Phi_m(L_x)}{dx} + |k_m|\,\Phi_m(L_x) = 4\pi\sigma_m(L_x), \tag{56}$$

so that after substituting the constants $\alpha_m(0) = \alpha_m(L_x) = |k_m|$, $\beta_m(0) = -1$, $\beta_m(L_x) = 1$, and $\gamma_m(0) = 4\pi\sigma_m(0)$, $\gamma_m(L_x) = 4\pi\sigma_m(L_x)$, one obtains the vacuum solution:

$$\Phi_m(x) = \psi_m(x) + \frac{1}{2|k_m|}\{\Pi_m - |k_m| P_m + 4\pi\sigma_m(L_x)\}\, e^{-|k_m|(L_x - x)}$$
$$- \frac{1}{2|k_m|}\{\Pi_m + |k_m| P_m - 4\pi\sigma_m(0)\}\, e^{-|k_m|x} \tag{57}$$

Note that we have the simplification $\chi_m{}^R(L_x - x) = \chi_m{}^L(x)$. The external surface charge at the boundaries oscillating at a prescribed frequency can serve as an external driver on the system. Since σ_{ext} is an arbitrary function of y, one can model a variety of external sources: grids, point sources, arrays of point sources, or capacitor plates of finite size.

For the case $m = 0$, we require the vacuum solutions to have continuous potentials and for the normal electric fields to be equal and opposite at plus and minus infinity. Thus

$$\Phi_0{}^v(x) = Ax + \Phi_0(0) \qquad x \leqslant 0, \tag{58}$$

$$\Phi_0{}^v(x) = A(L_x - x) + \Phi_0(L_x) \qquad x \geqslant L_x\,. \tag{59}$$

Requiring the jump in the normal electric field to equal the external surface charge density at the boundaries gives the conditions:

$$-\frac{d\Phi_0(0)}{dx} + A = 4\pi\sigma_0(0),$$

$$A + \frac{d\Phi_0(L_x)}{dx} = 4\pi\sigma_0(L_x).$$

The constant A can be determined from Gauss' Law by adding these equations. Thus the appropriate boundary constants are $\alpha_0(0) = 0$, $\alpha_0(L_x) = \beta_0(0) = \beta_0(L_x) = 1$, and

$$\gamma_0(0) = 2\pi\rho_{00}L_x + 2\pi\sigma_0(L_x) - 2\pi\sigma_0(0), \tag{60}$$

$$\gamma_0(L_x) = -2\pi\rho_{00}L_x + 2\pi\sigma_0(L_x) - 2\pi\sigma_0(0) + \Phi_0(L_x). \tag{61}$$

Substituting these into equation (31) leads to the solution:

$$\Phi_0(x) = \psi_0(x) + 2\pi\rho_{00}x(L_x - x) - [2\pi\sigma_0(L_x) - 2\pi\sigma_0(0) + \Pi_0](L_x - x) + \Phi_0(L_x) - P_0\,. \tag{62}$$

The solution is then determined to within the constant $\Phi_0(L_x)$.

It should be pointed out that the field boundaries for the potential calculation ($x = 0$, L_x) need not coincide with the plasma boundaries so long as they are outside the plasma. This allows one to model a plasma that forms its own boundary in vacuum, by fixing the field boundaries sufficiently far from the plasma. Hockney's technique [4] for solving the vacuum boundary value problem also uses Fourier series, but in this application his method requires twice as many Fourier modes than the method presented here.

5. *Vacuum specified at $x = 0$, potential at $x = L_x$.*

The appropriate constants in this case are: $\alpha_m(0) = |k_m|$, $\alpha_m(L_x) = 1$, $\beta_m(0) = -1$, $\beta_m(L_x) = 0$, and $\gamma_m(0) = 4\pi\sigma_m(0)$, $\gamma_m(L_x) = \phi_m(L_x)$, and the solution can be written in the form:

$$\Phi_m(x) = \psi_m(x) + [\phi_m(L_x) - P_m]\, e^{-|k_m|(L_x - x)} - \frac{1}{k_m}[\Pi_m + |k_m| P_m - 4\pi\sigma_m(0)]\, e^{-|k_m|L_x} \sinh[k_m(L_x - x)]. \tag{63}$$

For $m = 0$, equation (62) applies.

6. *Vacuum specified at $x = 0$, normal electric field at $x = L_x$.*

For this boundary condition, one has $\alpha_m(0) = |k_m|$, $\alpha_m(L_x) = 0$, $\beta_m(0) = \beta_m(L_x) = -1$, and $\gamma_m(0) = 4\pi\sigma_m(0)$, $\gamma_m(L_x) = \epsilon_m(L_x)$. The solution then simplifies to:

$$\Phi_m(x) = \psi_m(x) - \frac{1}{|k_m|}[\epsilon_m(L_x) - \Pi_m]\, e^{-|k_m|(L_x - x)} - \frac{1}{|k_m|}[\Pi_m + |k_m| P_m - 4\pi\sigma_m(0)]\, e^{-|k_m|L_x} \cosh[k_m(L_x - x)]. \tag{64}$$

For $m = 0$, the correct solution is given by equation (48). This solution can be used if

TABLE I[a]

1. Potential specified at $x = 0$, $x = L_x$
$A_m^x = -iA_m^y = -[k_m\phi_m(L_x) - k_mP_m]$ $B_m^x = iB_m^y = [k_m\phi_m(0) - k_mP_m]$ $f_m^x(x) = g_m^x(x) = \cosh(k_mx)/\sinh(k_mL_x)$ $f_m^y(x) = g_m^y(x) = \sinh(k_mx)/\sinh(k_mL_x)$ $BC_0 = -[\phi_0(L_x) - \phi_0(0)]/L_x + \Pi_0$
2. Normal electric field specified at $x = 0$, $x = L_x$
$A_m^x = -iA_m^y = [E_m(L_x) - \Pi_m]$ $B_m^x = iB_m^y = [E_m(0) - \Pi_m]$ $f_m^x(x) = g_m^x(x) = \sinh(k_mx)/\sinh(k_mL_x)$ $f_m^y(x) = g_m^y(x) = \cosh(k_mx)/\sinh(k_mL_x)$ $BC_0 = \epsilon_0(L_x) - 2\pi\rho_{00} \cdot L_x$
3. Potential specified at $x = 0$, normal electric field specified at $x = L_x$
$A_m^x = -iA_m^y = [\epsilon_m(L_x) - \Pi_m]$ $B_m^x = iB_m^y = [k_m\phi_m(0) - k_mP_m]$ $f_m^x(x) = g_m^y(x) = \cosh(k_mx)/\cosh(k_mL_x)$ $f_m^y(x) = g_m^x(x) = \sinh(k_m)/\cosh(k_mL_x)$ $BC_0 = \epsilon_0(L_x) - 2\pi\rho_{00} \cdot L_x$

[a] Boundary electric fields have the form

$$E_m^x(x) = \sum_{n=-\infty}^{\infty} -\frac{ik_n}{k_n^2 + k_m^2} 4\pi\rho_{nm}\, e^{ik_nx} + A_m^x f_m^x(x) + B_m^x g_m^x(L_x - x),$$

$$E_m^y(x) = \sum_{n=-\infty}^{\infty} -\frac{ik_m}{k_n^2 + k_m^2} 4\pi\rho_{nm}\, e^{ik_nx} + A_m^y f_m^y(x) + B_m^y g_m^y(L_x - x),$$

$$E_0^x(x) = \sum_{n=-\infty}^{\infty}{}' -\frac{i}{k_n} 4\pi\rho_{nm}\, e^{ik_nx} - 4\pi\rho_{00}\left(\frac{L_x}{2} - x\right) + BC_0 - \Pi_0,$$

$$E_0^y(x) = 0.$$

The constants A_m^i, B_m^i and the functions $f_m^i(x)$, $g_m^i(x)$ for each component i, along with the constant BC_0, are summarized in this Table.

Table continued

TABLE I—*Continued*

4. Vacuum specified at $x = 0$, $x = L_x$

$$A_m^x = -\frac{i\,|\,k_m\,|}{k_m} A_m^v = -\tfrac{1}{2}[\Pi_m - |\,k_m\,|\,P_m + 4\pi\sigma_m(L_x)]$$

$$B_m^x = \frac{i\,|\,k_m}{k_m} B_m^v = -\tfrac{1}{2}[\Pi_m + |\,k_m\,|\,P_m - 4\pi\sigma_m(0)]$$

$$f_m^x(x) = g_m^x(x) = f_m^v(x) = g_m^v(x) = e^{-|k_m|(L_x-x)}$$

$$BC_0 = -2\pi\sigma_0(L_x) + 2\pi\sigma_0(0)$$

5. Vacuum specified at $x = 0$, potential specified at $x = L_x$

$$A_m^x = -\frac{i\,|\,k_m\,|}{k} A_m^v = -\frac{|\,k_m\,|}{k}[k_m\phi_m(L_x) - k_m P_m]$$

$$B_m^x = iB_m^v = -[\Pi_m + |\,k_m\,|\,P_m - 4\pi\sigma_m(0)]$$

$$f_m^x(x) = f_m^v(x) = e^{-|k_m|(L_x-x)}$$

$$g_m^x(x) = e^{-|k_m|L_x}\cosh(k_m x)$$

$$g_m^v(x) = e^{-|k_m|L_x}\sinh(k_m x)$$

$$BC_0 = -2\pi\sigma_0(L_x) + 2\pi\sigma_0(0)$$

6. Vacuum specified at $x = 0$,
normal electric field specified at $x = L_x$

$$A_m^x = -\frac{i\,|\,k_m\,|}{k_m} A_m^v = [\epsilon_m(L_x) - \Pi_m]$$

$$B_m^x = iB_m^v = -\frac{k_m}{|\,k_m\,|}[\Pi_m + |\,k_m\,|\,P_m - 4\pi\sigma_m(0)]$$

$$f_m^x(x) = f_m^v(x) = e^{-|k_m|(L_x-x)}$$

$$g_m^x(x) = e^{-|k_m|L_x}\sinh(k_m x)$$

$$g_m^v(x) = e^{-|k_m|L_x}\cosh(k_m x)$$

$$BC_0 = \epsilon_0(L_x) - 2\pi\rho_{00}\cdot L_x$$

symmetry about the center of a slab can be assumed in some problem. One need simulate only half the system by requiring $\epsilon_m(L_x) = 0$ and reflecting particles elastically from the boundary at $x = L_x$.

In our simulation the components of the acceleration are calculated directly, and

therefore it is useful to summarize the electric field components in Table I, where all the fields can be written in the form

$$\mathbf{E}_m(x) = \sum_{n=-\infty}^{\infty} \mathbf{E}_{nm} e^{ik_n x} + \mathbf{BC}_m(x). \tag{65}$$

This method of solving Poisson's equation for a bounded slab is equally applicable to magnetostatic codes where the vector Poisson's equation must be solved. This has been done for an isolated slab by Lin and Dawson [10]. Finally, this method can be extended to three dimensions for a system which is periodic in two dimensions and bounded in the third, or reduced to one dimension by using the solutions derived for $m = 0$.

IV. Application to Finite-Size Particles

Each particle, with label j and charge q_j, is advanced according to the force at position $\mathbf{r}_j$:

$$\mathbf{F}_i = -q_j \nabla \Phi(r_j). \tag{66}$$

For finite-size particles, one must integrate over the charge distribution of the particle:

$$\mathbf{F}_j = -q_j \int_v S(|\mathbf{r} - \mathbf{r}_j|)\, \nabla \Phi(\mathbf{r})\, d^3r, \tag{67}$$

where $S(|\mathbf{r}|)$ is the shape factor which gives the charge distribution of a particle whose center is at the origin. The differentiation is done analytically (see Table I). One advantage of using Fourier series is that integrals such as (67) can be done by a convolution theorem. In the periodic direction, the integral is immediate:

$$\mathbf{F}_j = q_j L_y \sum_{m=-\infty}^{\infty} \int_0^{L_x} \mathbf{E}_m(x)\, S_{-m}(x - x_j)\, e^{ik_m y_j}\, dx, \tag{68}$$

where $\mathbf{E}_m(x)$ is given by (65) and $S_m(x)$ is the Fourier transform coefficient in the y direction of $S(x, y)$. Substituting (65) into (68) one can carry through part of the x integration by observing that

$$\int_0^{L_x} S_{-m}(x - x_j)\, e^{ik_n x}\, dx \simeq e^{ik_n x_j} S_{-n,-m} L_x, \tag{69}$$

where S_{nm} is the double Fourier transform of $S(x, y)$, if the particle is sufficiently far from the boundaries that its density is negligible there. The result is:

$$\mathbf{F}_j \simeq q_j L_x L_y \sum_{m,n=-\infty}^{\infty} \mathbf{E}_{nm} S_{-n,-m} e^{ik_n x_j} e^{ik_m y_j}$$

$$+ q_j L_y \sum_{m=-\infty}^{\infty} e^{ik_m y_j} \int_0^{L_x} \mathbf{BC}_m(x)\, S_{-m}(x - x_j)\, dx. \tag{70}$$

The remaining integral in (70) can be performed analytically or numerically and the results stored for fixed values of x_j. In practice, however, this may not be necessary, since for many of the particle shapes in use it is a valid approximation that

$$\int_0^{L_x} \mathbf{BC}_m(x)\, S_{-m}(x - x_j)\, dx \simeq \mathbf{BC}_m(x_j) \tag{71}$$

Furthermore, the finite-size particle is important for smoothing particle collisions and should not be important for the interaction of the particles with the smooth fields arising from the solution of Laplace's equation.

V. Computational Considerations

In evaluating the force, Fast Fourier Transforms are used; one, therefore, normalizes distances to the grid spacing, $\tilde{x} \equiv xN_x/L_x, \tilde{y} \equiv yN_y/L_y$, where N_x and N_y are the number of grid points in the $\tilde{x}$ and $\tilde{y}$ direction, respectively. The force is evaluated at integral values of $\tilde{x}$, $\tilde{y}$, the grid points, and interpolated between the grid points to give the force at the position of the particles $\tilde{x}_j, \tilde{y}_j$. The infinite Fourier sums are approximated by summing the index n from $-N_x/2 + 1$ to $N_x/2 - 1$ and the index m from $-N_y/2 + 1$ to $N_y/2 - 1$. The sums can be put in the form required by the FFT by noting that $\exp[-2\pi i n\tilde{x}/N_x] = \exp[2\pi i(N_x - n)\tilde{x}/N_x]$ for integer $\tilde{x}$. One stores the coefficients with negative index n in the location labled with index $N_x - 1 > n' > N_x/2 + 1$ according to the rule $n' = N_x + n$ and setting $f_{N_x/2,m} = 0$. The index m is treated similarly. With these rules (70) can be written:

$$\mathbf{F}(\tilde{x}, \tilde{y}) \simeq q_j L_x L_y \sum_{n=0}^{N_x-1} \sum_{m=0}^{N_y-1} \mathbf{E}_{nm} S^*_{nm} e^{i\tilde{k}_n\tilde{x}} e^{i\tilde{k}_m\tilde{y}} + q_j L_y \sum_{m=0}^{N_y-1} \mathbf{FB}_m(\tilde{x})\, e^{i\tilde{k}_m\tilde{y}}. \tag{72}$$

where $\tilde{k}_n \equiv k_n L_x/N_x = 2n\pi/N_x$, $\tilde{k}_m \equiv k_m L_y/N_y = 2m\pi/N_y$, $S_{-n,-m} = S^*_{nm}$, and where we define:

$$\mathbf{FB}_m(\tilde{x}) \equiv \int_0^{N_x} \mathbf{BC}_m(\tilde{x}')\, S_{-m}(\tilde{x}' - \tilde{x})\, d\tilde{x}'. \tag{73}$$

To evaluate (72) requires a two-dimensional FFT and a one-dimensional FFT for each value of $\tilde{x}$. Because $FB_m(x)$ is exponentially decreasing away from the boundaries, additional economies in the correction terms can be achieved: for increasing k_m, increasingly more terms in the interior are negligible and can be set to zero.

The force calculation can be optimized by combining the one- and two-dimensional FFT's into a single two-dimensional FFT. To do this one expands (73) as a discrete transform in the x direction:

$$\mathbf{FB}_{nm} \equiv \frac{1}{N_x} \sum_{\tilde{x}=0}^{N_x-1} \mathbf{FB}_m(\tilde{x})\, e^{-i\tilde{k}_n\tilde{x}}, \tag{74}$$

where $\tilde{x}$ takes on integer values. When this transform is inverted one recovers (73) at integral $\tilde{x}$ except that $\mathbf{FB}_m(N_x)$ is undefined by this method; however, equation (69) already assumed there were no particles there.

By substituting the expressions in Table I into (74), one can write the ith component of $\mathbf{FB}_{nm}$ in the form:

$$FB^i_{nm} = A_m{}^i f^i_{nm} + B_m{}^i g^i_{nm} , \tag{75}$$

where the constants $A_m{}^i$, $B_m{}^i$ contain the specific information about the boundary conditions that needs to be updated every time step, and the functional forms f^i_{nm}, g^i_{nm} depend only on the type of boundary conditions and can be stored after their initial calculation. The total force can be written in the following form:

$$\mathbf{F}(\tilde{x}, \tilde{y}) \approx q_j \sum_{n=0}^{N_x-1} \sum_{m=0}^{N_y-1} \{L_x L_y \mathbf{E}_{nm} S^*_{nm} + L_y \mathbf{FB}_{nm}\} e^{i\tilde{k}_n \tilde{x}} e^{i\tilde{k}_m \tilde{y}} \tag{76}$$

Note that the single FFT is actually used in two distinct ways in (76). First it is used as a discrete transform to represent the boundary terms at integer points. Secondly, it is used as a convenient technique for performing a partial Fourier sum. When the force is expressed in the form of (76), we have found that simulating a typical bounded system takes about 10 % more computing time than a similar doubly periodic system.

Some additional computational economy can be achieved for boundary conditions which are not of the mixed type (1, 2 and 4 in Table I), which have the property that $\chi_m{}^R(L_x - x) = \pm\chi_m{}^L(x)$. Observing the identity for $f_m(x)$ real,

$$\frac{1}{N_x} \sum_{\tilde{x}=0}^{N_x-1} f_m(N_x - \tilde{x})\, e^{-i\tilde{k}_n \tilde{x}} = \left[\frac{1}{N_x} \sum_{\tilde{x}=0}^{N_x-1} f_m(\tilde{x})\, e^{-i\tilde{k}_n \tilde{x}}\right]^* + \frac{f_m(N_x) - f_m(0)}{N_x} , \tag{77}$$

it follows that one can then write (75) in the following general form:

$$FB^i_{nm} = A_m{}^i f^i_{nm} + B_m{}^i [f^i_{nm}]^* + B_m{}^i C_m . \tag{78}$$

VI. Simulation of Waves in a Bounded Plasma

The computer model described here has been programmed in FORTRAN on UCLA's IBM 360/91 computer. An appropriate test of the model is to examine how successfully linear waves in a bounded plasma are simulated; in particular, we consider a plasma bounded on both sides by vacuum. An especially interesting type of linear wave that exists on a plasma-vacuum boundary is the surface wave, which was first observed experimentally in 1959 by Trivelpiece and Gould [11]. Many other authors have since derived the dispersion relation for surface waves in various limits and geometries. Using the model of a warm electron fluid and cold ions, and applying the

method of Andersson and Weissglas [12], one can obtain the following dispersion relation in slab geometry [13]:

$$1 - \frac{\omega_{pe}^2 + \omega_{pi}^2}{\omega^2} + \tanh\left(\frac{|k_y| L_x}{2}\right) - \frac{|k_y| \omega_{pe}^2}{\tau(\omega^2 - \omega_{pi}^2)} \tanh\left(\frac{\tau L_x}{2}\right) = 0, \quad (79)$$

for the anti-symmetric surface modes and

$$1 - \frac{\omega_{pe}^2 + \omega_{pi}^2}{\omega^2} + \coth\left(\frac{|k_y| L_x}{2}\right) - \frac{|k_y| \omega_{pe}^2}{\tau(\omega^2 - \omega_{pi}^2)} \coth\left(\frac{\tau L_x}{2}\right) = 0, \quad (80)$$

for the symmetric surface modes, where

$$\tau^2 \equiv k_y^2 + \frac{\omega_{pe}^2 + \omega_{pi}^2 - \omega^2}{\gamma_e v_{the}^2 (1 - (\omega_{pi}^2/\omega^2))}, \quad (81)$$

k_y is the wave number in the periodic direction, L_x is the width of the slab, ω_{pe}^2, ω_{pi}^2 are the electron and ion plasma frequencies, γ_e is the adiabatic constant, and $v_{the}^2 \equiv kT_e/M_e$ is the electron thermal velocity. For electron surface waves whose wavelength is small compared to the slab width, $k_y L_x \gg 1$, the two branches of the dispersion relation merge and the frequency ($\omega_{pi}^2 \ll \omega_{pe}^2$) is given by:

$$\omega = \frac{\omega_{pe}}{2}\{(2 + \gamma_e k_y^2 \lambda_{De}^2)^{1/2} + (\gamma_e)^{1/2} |k_y \lambda_{De}|\}, \quad (82)$$

where $\lambda_{De}^2 \equiv v_{the}^2/\omega_{pe}^2$. Ion surface waves also exist. For $k_y \lambda_{De} \ll 1$, there is only a symmetric mode with frequency slightly below $k_y c_s$. As $k_y \lambda_{De}$ increases an anti-symmetric ion surface wave also appears, and in the limit $k_y \lambda_{De} \gg 1$, the frequency of both modes approaches $\omega_{pi}/(2)^{1/2}$.

In addition to surface waves, propagating waves can exist in the body of a finite

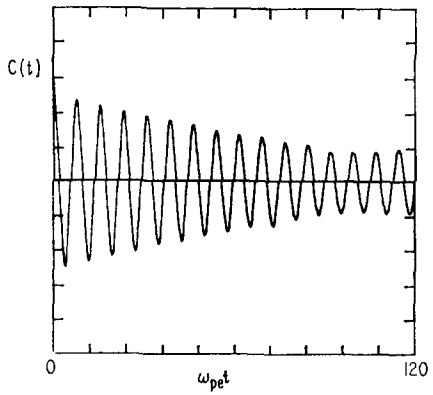

FIG. 1. Autocorrelation function of potential for anti-symmetric surface wave. ($m_e/M_i = 0$, $L_x/\lambda_{De} = 32$, $k_y L_y/2\pi = 2$, 32×128 grid, 28×128 particles, particle size $a_x = a_y = 1$, $\lambda_{De} = 1$).

plasma. These waves are related to the resonances observed in plasmas since the 1930's. The propagating waves satisfy the usual infinite plasma dispersion relations,

$$\omega^2 = \omega_{pe}^2 + \omega_{pi}^2 + \gamma_e(k_x^2 + k_y^2)\, v_{the}^2 \tag{83}$$

for electron plasma waves and

$$\omega^2 = \frac{(k_x^2 + k_y^2)\, c_s^2}{1 + (\omega_{pi}^2/\omega_{pe}^2) + \gamma_e(k_x^2 + k_y^2)\, \lambda_{De}^2} \tag{84}$$

for ion acoustic waves, where $c_s^2 \equiv \gamma_e KT_e/M_i$ is the ion acoustic speed and $k_x = (-\tau^2)^{1/2}$ is determined by (79) and (80). In general, there is one solution with $n\pi/L_x < k_x < (n+1)\,\pi/L_x$ for each integer n.

This dispersion relation was compared with simulation results by calculating the autocorrelation function $C_k(t)$ for the potential ϕ_k of the computer plasma in thermal equilibrium, defined by

$$C_k(t) \equiv \frac{1}{\quad} \sum^{N-t} \phi_k(\tau)\, \phi_k^*(t+\tau). \tag{85}$$

Particles were reflected elastically at the boundaries, and the length of each run was $600\,\omega_{pe}t$. Symmetric and anti-symmetric surface modes were observed by adding and subtracting potentials on opposite boundaries, respectively, and Fourier analyzing the result in the y direction. A typical autocorrelation function for an anti-symmetric surface mode is shown in Figure 1. The spectrum analysis for the same mode, shown in Figure 2, gives the frequency. Since the eigenfunctions for the body waves are not purely sinusoidal and since the wavelength in the non-periodic direction is not an integral multiple of the system width, the standard FFT technique to find a mode with a particular k_x generally gives a mixture of different body waves. The resolution can be improved by taking advantage of the known symmetries or form of the eigenfunctions [13]. The real parts of the frequencies for electron waves are compared with the predictions of fluid theory in Figure 3. The agreement is excellent.

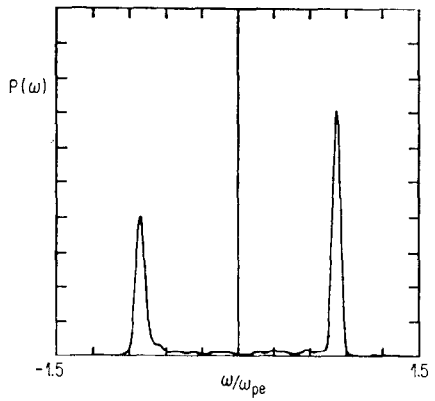

FIG. 2. Frequency analysis of autocorrelation function for anti-symmetric surface wave.

Using different mathematical techniques, the damping of the surface waves in the semi-infinite plasma limit has been calculated by Cheng and Harris [14] to be

$$|\gamma_s| = \omega_{pe}\left(\frac{2}{\pi}\right)^{1/2} k_y \lambda_{De} \tag{86}$$

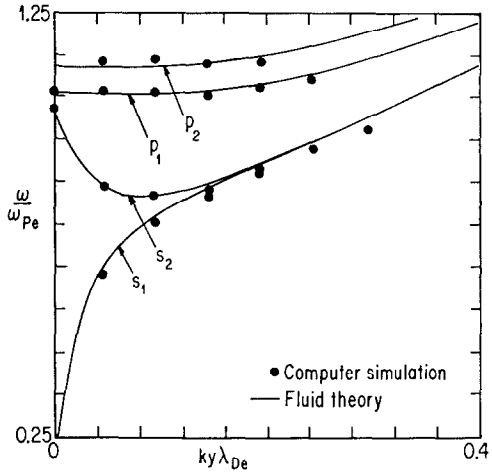

FIG. 3. Dispersion relation for electron waves calculated from fluid theory and simulation results. Curves S_1, S_2, correspond to symmetric and anti-symmetric surface waves, respectively, and P_1, P_2, to the longest wavelength symmetric and anti-symmetric propagating waves, respectively. ($m_e/M_i = 0$, $L_x\lambda_{De} = 32$, 32×128 grid, 28×128 particles, particle size $a_x = a_y = 1$, $\lambda_{De} = 1$).

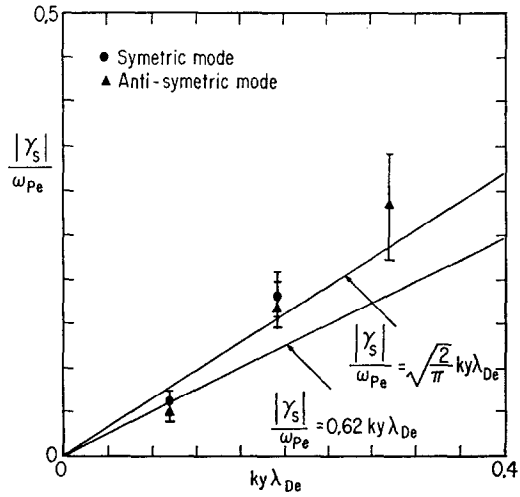

FIG. 4. Surface wave damping rate calculated from kinetic theory and simulation results. ($m_e/M_i = 0$, $L_x/\lambda_{De} = 32$, 64×128 grid, 60×128 particles, particle size $a_x = a_y = 1$, $\lambda_{De} = 2$).

and by Guernsey [15] to be:

$$|\gamma_s| = \omega_{pe} \times .62\, k_y \lambda_{De} \tag{87}$$

For the simulation parameters used, these expressions should be applicable for $k_y\lambda_{De} \gtrsim 1$. The simulation for surface wave damping, shown in Figure 4, indicate that the damping is proportional to $k_y\lambda_{De}$. Such a proportionality is expected if the

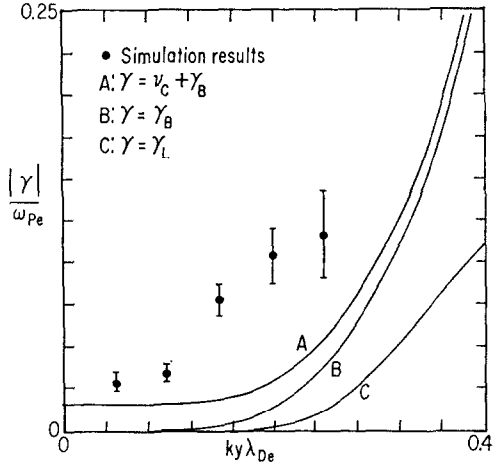

FIG. 5. Damping rate for longest wavelength symmetric electron plasma wave and simulation results. ($m_e/M_i = 0$, $L_x/\lambda_{De} = 32$, 32×128 grid, 28×128 particles, particle size $a_x = a_y = 1$, $\lambda_{De} = 1$).

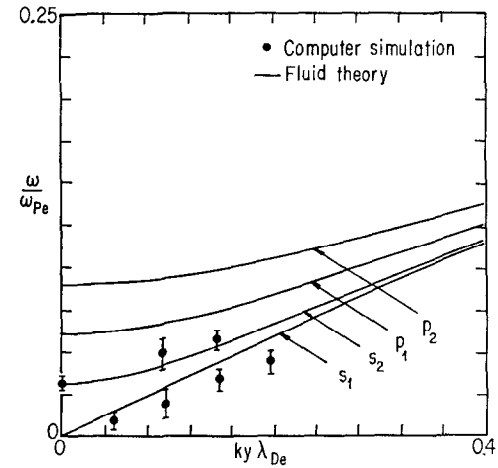

FIG. 6. Dispersion relation for ion waves calculated from fluid theory and simulation results. Curve S_1 corresponds to a symmetric surface wave, S_2 to an anti-symmetric wave which is propagating in the region shown, and P_1, P_2, to successively shorter wavelength symmetric and anti-symmetric propagating waves, respectively. ($m_e/M_i = 1/9$, $L_x/\lambda_{De} = 32$, 32×128 grid, $2 \times 28 \times 128$ particles, particle size $a_x = a_y = 1$, $T_e/T_i = 10$, $\lambda_{De} = 1$).

wave loses energy in reflecting from the warm plasma sheath at the boundary. This effect is like that of the well known anomalous skin effect in solid state [16] and arises because particles enter and leave the oscillating sheath layer at different phases of the oscillation, and on the average they gain energy. The results tend to favor the theory of Cheng and Harris.

Cheng and Harris [14] also calculate an approximate expression for the damping of electron plasma (body) waves in a slab geometry. The Landau damping γ_B in a bounded plasma is increased from the usual infinite plasma damping γ_L, again due to the production of an oscillating sheath layer as the wave reflects from the boundary. The simulation results, shown in Figure 5, for the longest wavelength mode show a damping which is larger than predicted. The collisional damping ν_c based on an infinite plasma of finite-size particles [17] improves the fit considerably, but is not large enough to account for this difference in the simulation results. This indicates either the theory is incorrect, that it does not accurately account for our model consisting of finite-size particles, or that collisional damping is enhanced in a bounded plasma, probably due to enhanced collision rates associated with the sheath regions.

For ion waves the results are shown in Figure 6, and the real parts of the frequencies are in good agreement with the predictions of fluid theory for the lowest order modes. The run was not long enough to measure damping with any accuracy in this case.

VII. Remarks on Energy Conservation

The bounded plasma model described here does not, in general, conserve energy as well as similar doubly periodic models. Energy growth is linear in time and depends on the type of boundary condition used. The worst case of the ones tested was found to be the vacuum boundary condition, where for the run of Figure 3, energy growth was 0.8 % for $600\,\omega_{pe}t$. The best energy conservation occurred for zero potential at the boundaries (conducting walls).

In addition, it was found that collisions between cold ions and hot electrons give rise to further energy growth. This effect is reduced by increasing the ion-electron mass ratio and decreased as the two species came closer to equilibrium. This effect also depends on the type of boundary condition used. In a series of test runs, it was found that the energy conservation with the vacuum boundary conditions was about 3–5 times worse than for similar runs done with the standard doubly periodic codes. It was felt that the accuracy was sufficient for most investigations; however, the mechanism whereby the algorithm fails to conserve energy is one for further study.

VIII. Conclusion

In order to study problems in plasma physics where boundary conditions are important, a computer model to simulate a plasma slab is developed. The two-dimensional electrostatic particle model is periodic in one dimension and a variety of

boundary conditions can be handled in the other dimension. The boundary algorithm can be added, without major modifications, to existing doubly periodic models which solve Poisson's equation with Fourier series, and the additional time required for the boundary calculation can be made small. The computer model is tested by examining the dispersion of linear waves in a plasma slab bounded by vacuum, and comparing the simulation results with the predictions of a warm fluid theory, both for electron and ion waves. The agreement is very good. The damping of surface waves agrees favorably with a kinetic theory, while the damping of body waves is somewhat larger than can be accounted for with present theories.

ACKNOWLEDGMENT

We would like to thank Dr. Alfredo Banos, Jr., for his help in the formulation of the boundary value problem. Dr. Anthony Lin, Chih-Chien Lin, and Charles Thorington contributed to the development, debugging and testing of the computer model. This work was supported by the U.S.D.O.E. contract EY-76-C-03-0010 PA 26/Task III.

REFERENCES

1. C. K. BIRDSALL AND D. FUSS, *J. Computational Phys.* **3** (1969), 494.
2. W. L. KRUER, J. M. DAWSON, AND B. ROSEN, *J. Computational Phys.* **13** (1973), 114.
3. J. W. COOLEY AND J. W. TUKEY, *Math. Comp.* **19** (1965), 297.
4. R. W. HOCKNEY, *in* "Methods in Computational Physics," (B. Alder, S. Fernbach and M. Rotenburg, Eds.), Vol. 9, p. 135, Academic Press, New York, 1970.
5. D. POTTER, "Computational Physics," p. 80, Wiley, New York, 1973.
6. O. BUNEMAN, *in* "Proceedings of the Fourth Conference on Numerical Simulation of Plasma" (Boris and Shanny, Eds.), p. 642, U.S. Govt. Printing Office, Washington, D.C. (Stock No. 0851 0059), 1970.
7. A. B. LANGDON AND B. LASINSKI, *in* "Methods in Computational Physics (B. Alder, S. Fernbach, and M. Rotenburg, Eds.), Vol. 16, p. 339, Academic Press, New York, 1976.
8. O. BUNEMAN, *J. Computational Phys.* **12** (1973), 124.
9. J. M. DAWSON, H. OKUDA, AND B. ROSEN, *in* "Methods in Computational Physics" (B. Alder, S. Bernbach, and M. Rotenburg, Eds.), Vol. 16, p. 282, Academic Press, New York, 1976.
10. A. T. LIN AND J. M. DAWSON, *Phys. Fluids* **21** (1978), 109.
11. A. W. TRIVELPIECE AND R. W. GOULD, *J. Appl. Phys.* **30** (1959), 1784.
12. B. ANDERSON AND P. WEISSGLAS, *Phys. Fluids* **9** (1966), 271.
13. V. K. DECYK, Ph.D. Thesis, UCLA, 1977.
14. C. C. CHENG AND E. G. HARRIS, *Phys. Fluids* **12** (1969), 1262.
15. R. L. GUERNSEY, *Phys. Fluids* **12** (1969), 1852.
16. T. HOLSTEIN, *Phys. Rev.* **88** (1952), 1427.
17. H. OKUDA AND C. K. BIRDSALL, *Phys. Fluids* **13** (1970), 2123.